Astronomical and Astrophysical Transactions, 1998, Vol. 15, pp. 143–151
Reprints available directly from the publisher
Photocopying permitted by license only

PHOTOGRAPHIC OBSERVATIONS OF THE NOVA-LIKE VARIABLE V SGE

V. I. MARSAKOVA

Department of Astronomy, Odessa State University, T. G. Shevchenko Park, Odessa, 270014, Ukraine

(Received June 4, 1996)

V Sge was studied on 277 photonegatives of the Moscow and Odessa plate collections covering the interval JD 2 414 309–48 884. The total range is $10^m.05$–$13^m.28$ with a mean brightness $11^m.53$. The normal distribution approximation may be applied to the intensity rather than to brightness. Slow variations are not periodic showing peaks at the periodogram at 920^d, 61^d and 215^d, contrary to the published values 550^d and 249^d. The cycle length underwent changes. The best "running parabolae" fits correspond to the filter half width Δt from 25^d to 50^d. The orbital variations are blended by physical variability of the system.

KEY WORDS Cataclysmic stars, V Sge

1 INTRODUCTION

V Sge is one of the most attracting CVs. Being very bright ($8^m.6$–$13^m.9$, Kholopov *et al.*, 1987), it was discovered at the beginning of the century. The light variations were classified as irregular and separated in to slow waves with a cycle length from 100^d to 600^d and amplitude of $\approx 3^m$ and more rapid fluctuations of $\approx 2^m$ during a few days. Herbig *et al.* (1965) discussed these previous findings and have discovered regular eclipses and estimated the orbital period $P_{\rm orb} = 0^d.514195$ and proposed a model based on photoelectric and spectral data. Their value was slightly corrected ($P_{\rm orb} = 0^d.514198$) by Koch *et al.* (1986). Smak (1995) has found its secular decrease with a rate $dP/dt = -4.8 \times 10^{-10}$. The Catalogue by Aslanov *et al.* (1979) also mentioned the fast coherent (47.7 s) oscillations (Patterson, 1977) and a slow photometric cycle of 550^d.

Recent interest the object is partially connected with observational and theoretical study of the winds from the accretion disks in cataclysmic variables (Vitello and Shlosman, 1993; Mauche, 1994; Nafar *et al.*, 1992). Herbig *et al.* (1965) estimated the masses of the primary and secondary $M_1 = 0.74M_\odot$ and $M_2 = 2.8M_\odot$. Koch *et al.* (1986) proposed a model according to which the primary is a helium star filling its Roche lobe and the secondary is a neutron star surrounded by the accretion

disk. In 1995 an international campaign for photometric observations of this star was initiated by Hric *et al.* (1996).

In this paper we discuss the results of photographic photometry only. One may find analysis of the *UBV* photoelectric observations and the AFOEV visual estimates in Marsakova *et al.* (1996).

2 OBSERVATIONS

Observations were made on 211 plates of the State Sternberg Astronomical Institute (SAI) and 66 plates of the Astronomical Observatory of the Odessa State University (AO OSU). In both cases the emulsion ORWO ZU-21 was used, thus only minor differences between the instrumental systems are found. The time interval covered is JD 2 414 309–48 091 and 2 440 827–48 884, respectively. The *UBV* magnitudes of the comparison stars were obtained by S. Yu. Shugarov (Marsakova *et al.*, 1996).

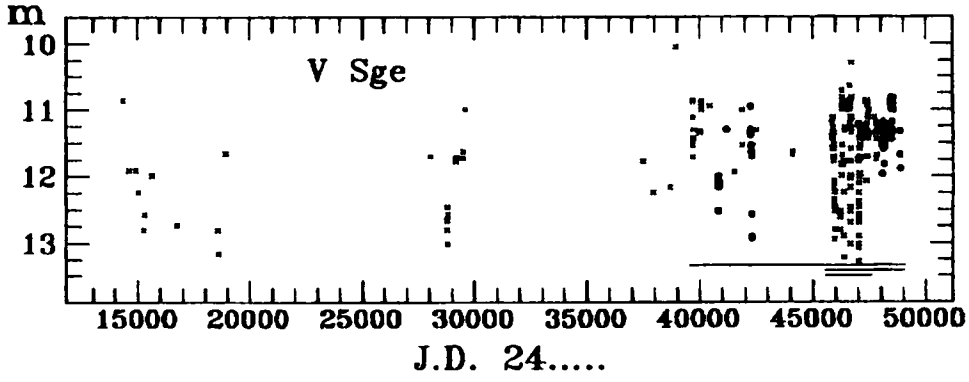

Figure 1 The composite photographic light curve of V Sge. Crosses correspond to the SAI plates, filled circles to the AO OSU plates. Horizontal lines show decreasing subintervals used for periodogram analysis: "a": JD 2 439 683–48 884 (top, $n = 246$), "b": 2 445 848–48 884 (middle, $n = 203$), "c": 2 445 848–47 092 (bottom, $n = 126$).

The composite light curve for Moscow and Odessa is shown in Figure 1. One may see apparent slow brightness variations superimposed on the more rapid changes. The range of the brightness variations is $10^m.64$–$13^m.28$ with two sure exceptions: $10^m.05$ (HJD 2 438 942.416) and $10^m.29$ (HJD 2 446 728.222). The mean brightness is $11^m.53 \pm 0^m.03$, the r.m.s. deviation from the mean is $\sigma = 0^m.62 \pm 0^m.03$. The asymmetry $A = \langle (m - \langle m \rangle)^3 \rangle / \sigma^3 = 0.542$ is positive and relatively large; the excess $E = \langle (m - \langle m \rangle)^4 \rangle / \sigma^4 - 3 = -0.403$ is negative and also large, challenging the hypothesis of a normal distribution.

The histogram of the brightness distribution is shown in Figure 2 with a fit "1" corresponding to the normal distribution with the mean and variance equal to the observed ones. The median of the distribution is equal to $11^m.53$ and is marked by

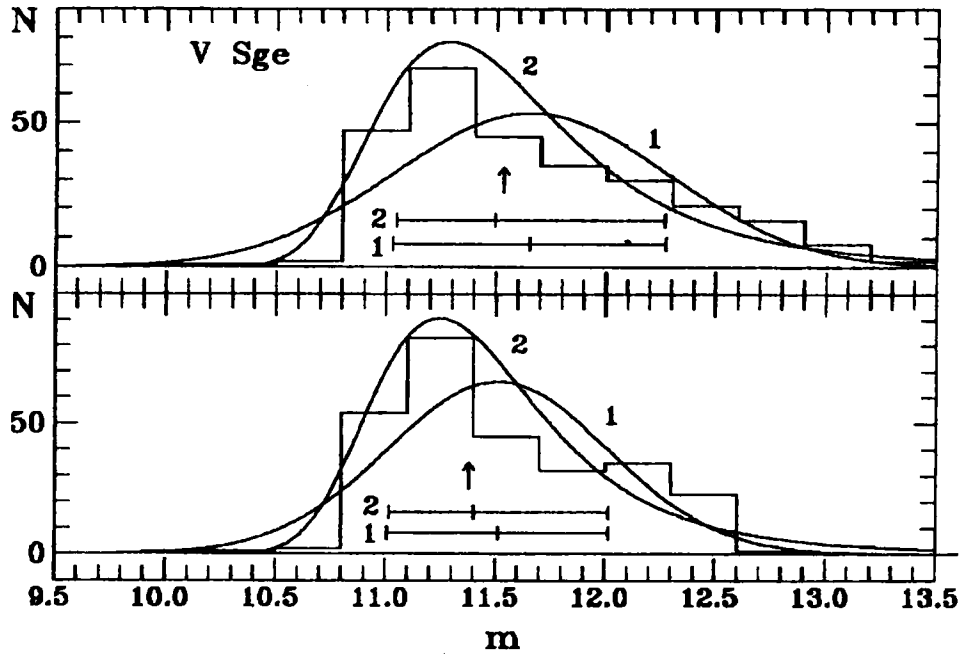

Figure 2 The histogram of the 277 photographic brightness estimates of V Sge. The vertical arrow corresponds to the median of the distribution, the line "1" to the normal distribution fit to the brightness; the line "2" to the normal distribution fit to the intensity. Vertical bars at horizontal lines correspond to the values of brightness $\langle m \rangle$, $\langle m \rangle \pm \sigma_m$ ("1") and $\langle I \rangle$, $\langle I \rangle \pm \sigma_I$ ("2").

a vertical arrow. One may see that the histogram has an asymmetric shape which may not be fitted by the normal distribution.

The second hypothesis we check is that the normal distribution may correspond to the *intensity I* rather than the *brightness m*. The values of the brightness corresponding to the mean intensity are $11^m.49 \pm 0^m.03$ and to the relative r.m.s. deviation $0^m.45 \pm 0^m.04$. One may see that the fit "2" corresponding to the approximation of the intensity distribution by the normal distribution fits the histogram much better than the curve "1". However, there is a deficiency of data points in the range $11^m.1$–$12^m.0$ and a corresponding excess of measurements fainter than $12^m.0$. This may indirectly argue for an amplitude-limited component of the variations, e.g. orbital and/or (quasi-)periodic luminosity changes.

3 CORRECTIONS OWING TO ORBITAL VARIABILITY

As the eclipses of V Sge are superimposed on to physical variability, we tried to remove their influence and to obtain "reduced" values of the maximum brightness.

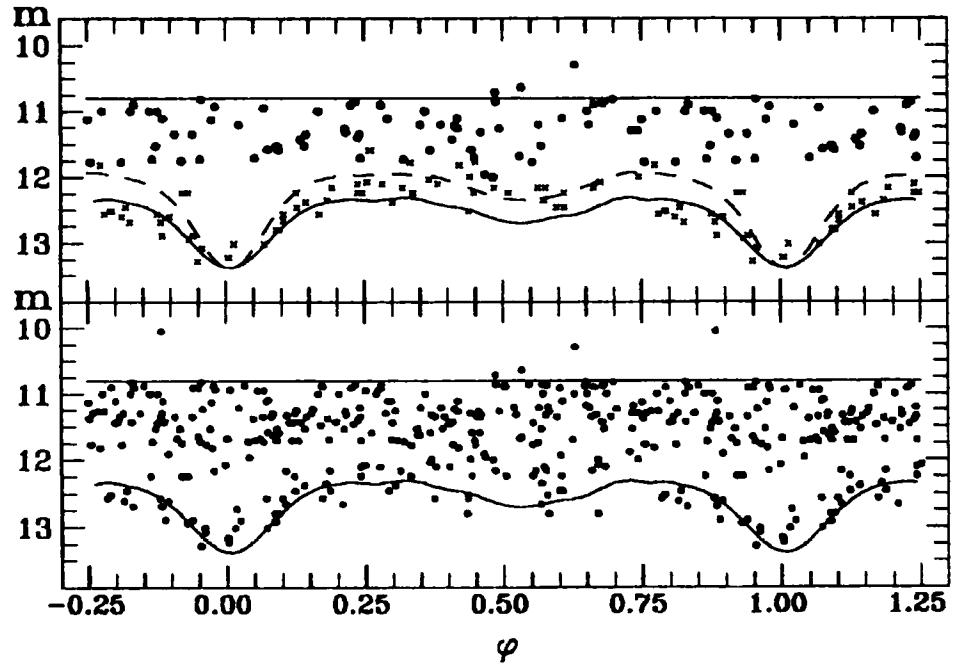

Figure 3 Phase light curve for "low" and "intermediate" luminosity states (top) and for all observations (bottom). The solid line is a photoelectric phase curve *scaled* to the inactive state; the dashed line is a photoelectric phase curve *shifted* at a constant intensity difference. The horizontal line corresponds to the "limiting" light curve with zero amplitude.

For this purpose we have plotted our data on to the phase curve shown in Figure 3. The phases were computed according to the ephemeris of Smak (1995)

$$\text{Min1} = 2437889.9157 + 0.51419706 \cdot E - 1.23 \times 10^{-10} \cdot E^2 \qquad (1)$$

where we used the moment of observation as the left part and (cycle number + phase) instead of E.

The phase curve is very noisy so we could not determine a valuable smoothing function. The peak of the periodogram computed by using the program FOUR-0 by Andronov (1994) near the orbital value is lower than a lot of nearby peaks caused by physical variability. Our analysis of the data in small time intervals corresponding to nearly the same luminosity states leads to the conclusion that the amplitude decreases towards high luminosity states; thus one has to model the luminosity dependence of the phase curve. A few nights corresponding to the lowest state were not sufficient to cover the whole phase interval, and we have used the mean photoelectric curve obtained for one luminosity state by Marsakova *et al.* (1996) as the "standard" one. The first approach often used is to subtract from the original observation the brightness of the "standard" curve. In this case the phase for the residuals showed an apparent maximum near phase 0 as the eclipse depth

is overestimated. A similar situation occurred when we transferred magnitudes to relative intensities. In this case, the amplitude of the "standard" curve increases with decreasing luminosity more rapidly than our observations show. Thus we have rejected both these hypotheses.

The next approach was to separate the lowest state and to compute the coefficients of the linear fit $m_{i,*} - \langle m_* \rangle = b \cdot (m_{st}(\phi_i) - \langle m_{st} \rangle)$, where $m_{i,*}$ is the photographic magnitude and $m_{st}(\phi_i)$ is the value at the standard curve at the same phase. The mean values are $\langle m_* \rangle = 12^m.68$ and $\langle m_{st} \rangle = 11^m.75$ and the slope is $b = 1.45 \pm 0.18$. Assuming a linear increase of the amplitude with mean magnitude one may easily obtain the brightness level $m_0 = 9^m.77$ corresponding to zero amplitude. In this very formal model one may obtain a parameter $\alpha_i = (m_i - m_0)/(m_*(\phi_1) - m_0)$ and a "reduced" brightness at maximum $m_{i,r} = m_0 + \alpha_i \cdot (m_{\max,*} - m_0)$. In fact for the analysis one may use the parameter α_i itself, and the last linear transform to formal "maximum brightness" is needed to deal with the more usual parameter – magnitude.

The phase curve for such "reduced" data again has a formal maximum near phase 0 because, according to our observations, the amplitude decreases to nearly zero at $m_0 = 10^m.8$ and the difference between the mean photographic and photoelectric magnitude is affected not only by the difference in the luminosity states, but also by a shift owing to the difference between the instrumental systems. As the *UBV* curves are highly correlated, the shape of the phase curve must not differ for pg and ph magnitudes, but a linear transformation is possible. Finally, we have chosen the value $m_0 = 10^m.8$ to avoid any significant phase dependence of the reduced data. The corresponding r.m.s. deviation from the mean decreased from $0^m.62$ for "initial" data to $0^m.50$ for the "reduced" data. The maximum amplitude of the "reduced" data for one night is $0^m.33$. As one may not expect significant luminosity changes during a few hours, this value characterizes the accuracy of photographic observations. The "reduced" data were used for further analysis to check differences in the results owing to orbital variability.

The histogram of the reduced brightness and intensity is shown in Figure 2. The mean brightness is $11^m.51$; $\sigma = 0^m.50$, and the asymmetry is $A = 0.381$. The median of the distribution is $11^m.39$. The brightness corresponding to the mean intensity is equal to $11^m.40$, $\sigma = 0^m.39$, also closer to the median than $\langle m \rangle$, as for the initial data. However, the deviation of the distribution from the normal one is still significant; it is also smaller for the reduced data than for the initial ones.

The resulting approximating phase curve for minimal luminosity ($\alpha = 1$) is shown in Figure 3. For comparison we show a phase curve obtained from the photoelectric one by subtracting constant intensity at a value corresponding to the magnitude at mid-eclipse, which is equal to the "reduced" one for $\alpha = 1$.

4 PERIODOGRAM ANALYSIS

For the analysis we have chosen the whole observational interval and three subintervals marked in Figure 1 by horizontal lines. The two brightenings mentioned above were removed from the subinterval runs to reduce bias of the results.

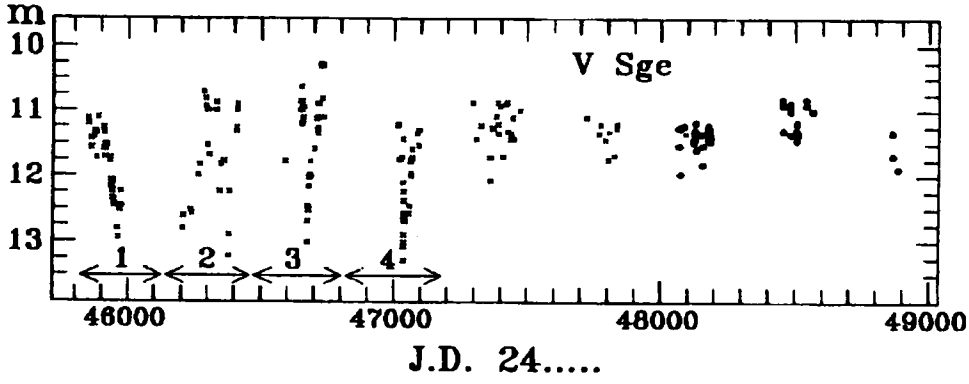

Figure 4 The photographic light curve of V Sge in the best covered time subinterval "b". Filled squares correspond to a possible brightening not taken into account for periodogram analysis. The subintervals "1"–"4" are shown separately in Figure 7; their sum is the smallest subinterval "c" used for periodogram analysis.

We have used the one-harmonic approximation for each trial period and computed a periodogram $S(f) = \sigma_C^2/\sigma_O^2$ by using the program FOUR-0 by Andronov (1994). Here σ_O and σ_C are r.m.s. deviations of the observed (O) and calculated (C) values from the mean. The corresponding periodograms are shown in Figure 5. One may note a few peaks in the periodograms which have similar height. The characteristics of the highest peaks, including the best fit period P_1 and amplitude r_1, are listed in Table 1. The "false alarm probability", i.e. the probability of obtaining a peak of given height at one of the "independent frequencies" if the data are pure white noise (cf. Terebizh, 1992; Andronov, 1994, 1996), is equal to 10^{-L_p}.

The values of L_p are very large justifying the conclusion that the signal is not really white noise. However, such a complex structure of the periodogram may be due to the cycle length changing with time and to the influence of a "spectral window".

The periodograms were also computed for the resuduals of the observations from the best sine fit. The corresponding amplitude r_2 and period P_2 are also listed in Table 1. The values appearing more than once are $\approx 920^d$, 60.6^d and $\approx 210^d$.

Table 1. Characteristics of the highest peaks of the periodogram

run	n	$\langle m \rangle$	σ_m	$S(f)$	L_p	P_1	r_1	r_2	P_2
0i	277	11.65	0.619	0.188	9.3	913.8 ± 2.0	411 ± 51	324	36.7
ai	246	11.60	0.586	0.211	9.9	72.99 ± .05	379 ± 47	301	221.0
bi	203	11.61	0.591	0.250	10.4	922.9 ± 16.	459 ± 57	303	36.7
ci	126	11.79	0.653	0.449	14.2	60.57 ± .11	652 ± 67	393	208.0
0r	277	11.51	0.500	0.201	10.4	214.8 ± .11	321 ± 39	272	40.8
ar	246	11.48	0.472	0.225	10.9	896.0 ± 4.6	374 ± 43	266	91.2
br	203	11.48	0.482	0.280	12.2	928.6 ± 16.	393 ± 46	262	37.7
cr	126	11.64	0.530	0.455	14.5	60.63 ± .11	530 ± 54	313	210.0

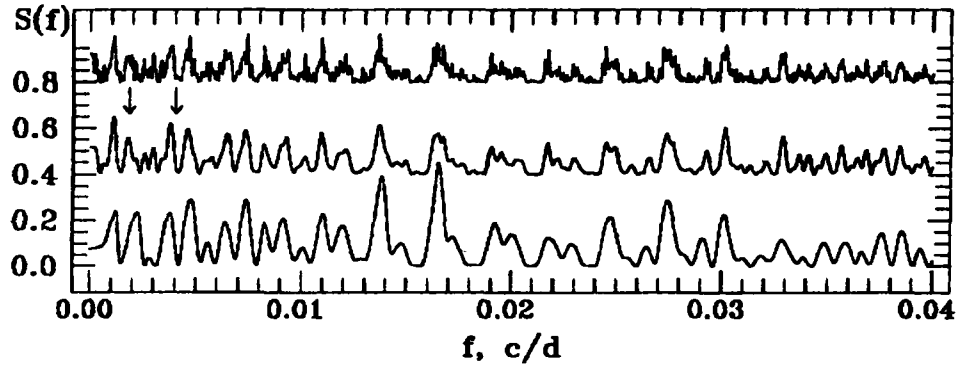

Figure 5 Test functions S_F for one harmonic for the decreasing subintervals "a", "b", "c" (top to bottom). Vertical arrows correspond to the suspected "periods" 550^d and 246^d, respectively.

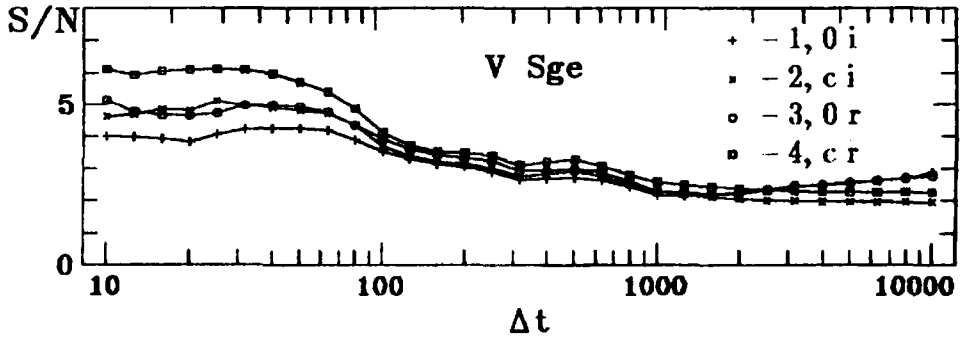

Figure 6 Signal-to-noise ratio for the "running parabolae" fits vs. filter half-width Δt for initial ("i", 1,2) and reduced ("r", 3,4) data in the subintervals "0" (1,2) and "c" (2,4).

5 ANALYSIS USING THE METHOD OF "RUNNING PARABOLAE"

As discussed above, the variations of luminosity are aperiodic and we used another method to estimate the characteristic time scale. The "running parabolae" fit (Andronov, 1990) was used with a number of trial values of the filter half-width Δt ranging from 1^d to 10000^d. As expected from theoretical models, with increasing values of Δt the r.m.s. deviation of the observations from the fit σ_{O-C} increases, the mean number of observations located within the filter width increases leading to a decrease of the r.m.s. value of the error estimate of the fit at the time of observation. The last parameter we may use as "noise". The r.m.s. amplitude σ_C of the fit ("signal") decreases. Thus the "signal/noise" (S/N) ratio has a well-pronounced maximum for signals with cyclic shape. For periodic signals, $\Delta t_{max} = 0.5450P$.

The dependence of S/N on Δt is shown in Figure 6 for initial and reduced data. Contrary to periodic signals, the maximum is very wide; the values rapidly decrease for $\Delta t \leq 100^d$. For $\Delta t < 10^d$ the number of observations located within

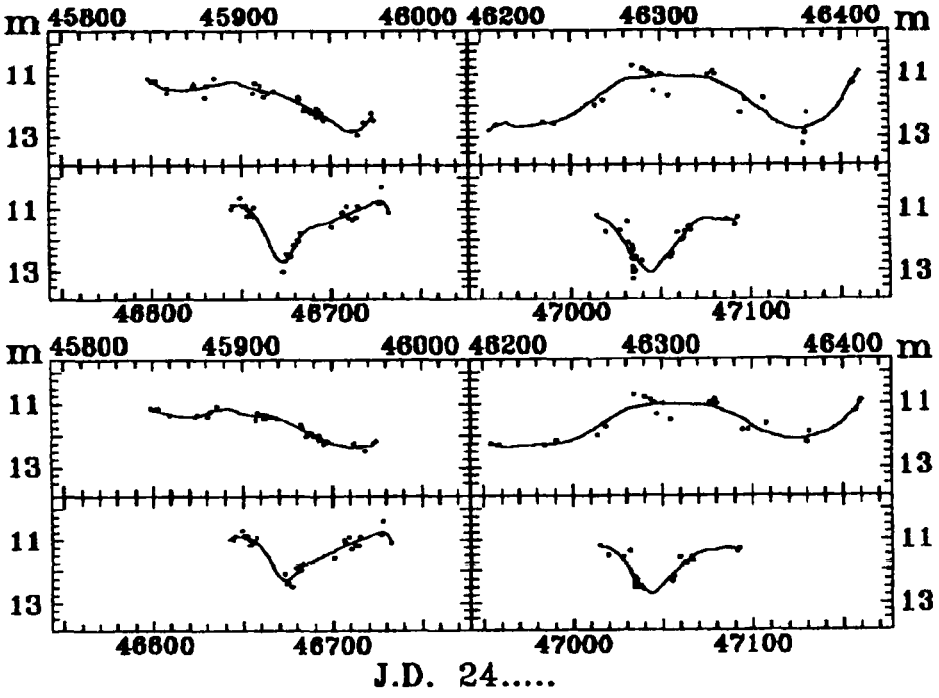

Figure 7 Light curves for the initial (top) and reduced (bottom) data in subinterval "c" and their "running parabolae" fits with $\Delta t = 25^d$. For the interval 46200–46400 the value $\Delta t = 50^d$ was adopted bacause of larger gaps between the observations.

the filter width is much smaller, thus the curves become unstable. For the adopted interval of Δt, the maxima of S/N occur at 25^d (both initial and reduced data in the subinterval "b") and at 39–50^d for the whole interval. The maximum values S/N_{max} reach 6 (reduced data in subinterval "c") and are smaller for the initial data than for reduced data (owing to the contribution of much faster orbital variability) and for the whole interval than for the subinterval "c" (owing to higher amplitude and more prominent cyclicity).

The light curves for four seasons within subinterval "c" are shown in Figure 7. They exhibit apparent variations of luminosity at time scales 50–150^d. The influence of the orbital variability on the light curve at larger time scales is clearly seen.

6 CONCLUSIONS

Although the orbital variability is significant, it is blended by larger luminosity changes forbidding us to determine the phase curve. The reduction of the data in the frame of the hypothesis of constant shape and amplitude linearly dependent on the mean brightness allows us to decrease the scatter of the light curve and study the variations with higher signal-to-noise ratio.

The periodogram at low frequencies exhibits a variety of peaks with a height ratio changing with the width of the subinterval. The long-term changes are apparently seen at a cycle length 900^d, but in the smaller subinterval "c" the variations are much faster, and the highest peak of the periodogram occurs at 60.6^d. Another peak is observed at a timescale close to the value 248.7 ± 0.2^d derived from the AFOEV observations (Marsakova *et al.*, 1996). The number of photographic observations is smaller than of the AFOEV ones, but they are homogeneous, obtained by using the same emulsion, and thus the transitions between maximal and minimal brightness are well pronounced, as one may see in Figure 7. Thus the derived "cycle length" values may be interpreted as a characteristic time of irregular variations rather than the duration of the quasi-periodic oscillations. The aperiodic fluctuations are best fitted by a "running parabolae" approximation with a filter half-width Δt ranging from 25^d to 50^d.

Continuation of the monitoring is needed to study the character of the luminosity variations of this interesting object.

Acknowledgements

The author is grateful to I. L. Andronov, S. Yu. Shugarov and M. A. Voronkov for helpful discussions and to the Astronomical Society for a travel grant. The work was partially supported by the Ukrainian State Committee for Science and Technique (DKNT).

References

Andronov, I. L. (1990) *Kinematika Fiz. Neb. Tel.* **6**, 87.
Andronov, I. L. (1994) *Odessa Astron. Publ.* **7**, 49.
Andronov, I. L. (1996) *Space Sci. Rev.*, submitted.
Aslanov, A. A., Kolosov, D. E., Lipunova, N. A., Khruzina, T. S., and Cherepashchuk, A. M. (1989) *Catalogue of Close Binary Stars at Late Evolutionary Stages*, Moscow University Press, 240pp. (in Russian).
Herbig, G. H., Preston, G. W., Smak, J., and Paczynski, B. (1965) *Astrophys. J.* **141**, 617.
Hric, L., Petrik, K., and Urban, Z. (1996) In *Cataclysmic Variables and Related Objects*, J. Wood (ed.) (in press).
Kholopov, P. N., Samus', N. N., Frolov, M. S., Goranskij, V. P., Gorynya, N. A., Karitskaya, E. A., Kazarovets, E. V., Kireeva, N. N., Kukarkina, N. P., Medvedeva, G. I., Pastukhova, E. N., Perova, N. B., and Shugarov, S. Yu. (1987) *General Catalogue of Variable Stars*, 4th ed. **3**, 368pp.
Koch, R. H., Colcoran, M. F., Holenstein, B. D., and McCluskey, Jr. G. E. (1986) *Astrophys. J.* **306**, 618.
Marsakova, V. I., Andronov, I. L., Schweitzer, E., Shugarov, S. Yu., and Voronkov, M. A. (1996) in preparation.
Mauche, C. (1994) In *Interacting Binary Stars, A. S. P. Conf. Ser.* **56**, 74.
Nafar, I., Shaviv, G., and Wehrse, R. (1992) In *Viña del Mar Workshop on Cataclysmic Variable Stars, A. S. P. Conf. Ser.* **29**, 65.
Patterson, J. (1977) *IAU Circ.* **3134**.
Smak, J. (1995) *Acta Astr.* **45**, 361.
Terebizh, V. Yu. (1992) *Time Series Analysis in Astrophysics*, Moscow, 392pp. (in Russian).
Vitello, P. and Shlosman, I. (1993) *Astrophys. J.* **410**, 815.